International Journal for Multidisciplinary Research (IJFMR)
E-ISSN: 2582-2160 ● Website: www.ijfmr.com ● Email: editor@ijfmr.com

Enhancement of CSIFT Algorithm for Improved Feature Extraction in Psoriasis Image Analysis

Aiyanne Yori Q. Perdigon[1], Julianne Cyrille T. Rico[2], Raymund M. Dioses[3], Khatalyn E. Mata[4]

[1,2]Student, College of Information Systems Technology Management Department, Pamantasan ng Lungsod ng Maynila
[3,4]Faculty, College of Information Systems Technology Management Department, Pamantasan ng Lungsod ng Maynila

Abstract
The precise extraction of lesion features for psoriasis analysis is frequently hindered by the computational latency and "feature blindness" inherent in standard image processing algorithms, which often struggle to capture the subtle texture of organic skin lesions. Addressing the critical trade-off between execution efficiency and diagnostic sensitivity, an Enhanced Color Scale-Invariant Feature Transform (CSIFT) was engineered to optimize the feature extraction architecture for dermatological analysis through three pivotal technical interventions: the replacement of iterative pixel-wise computations with Vectorized Matrix Operations, the implementation of a Texture-Aware Detection module utilizing Adaptive Cr-Otsu Masking with Hybrid Harris Corner detection, and the integration of RootSIFT Normalization. Comparative performance analysis revealed a transformative improvement over the Standard method, as the proposed vectorization strategy achieved an 83.62% reduction in processing overhead, lowering the average execution time from 15,962.29 ms to 2,615.38 ms. Furthermore, the system resolved the loss of low-contrast details, recording a 218% increase in keypoint density from an average of 200.82 to 639.97 points while simultaneously improving the Matching Score to 97.06% compared to the Standard model's 61.00%. These findings confirm that the Enhanced CSIFT provides a mathematically robust, accurate solution for dermatological imaging, effectively bridging the gap between computational speed and the precision required for clinical assessment.

Keywords: Color Scale-Invariant Feature Transform, Feature Extraction, Psoriasis

1. Introduction

1.1. Background of the Study

Psoriasis is a chronic, immune-mediated skin disorder marked by inflamed, red, and scaly plaques. It affects approximately 125 million people globally, or about 2.2–3% of the population, making it one of the most prevalent dermatological conditions worldwide (Smith, 2021). The Global Burden of Disease study in 2019 reported over 40 million prevalent cases, with significant physical, psychological, and economic consequences with an age-standardized rate of 503.6 per 100,000 people globally (Damiani et al., 2021). A substantial proportion of patients, around 10–30% also develop psoriatic arthritis, a painful condition that further compromises mobility and quality of life (Pratt, 2025).

While psoriasis prevalence is highest in high-income regions such as Western Europe and North America with age-standardized rates exceeding 1,000 per 100,000 people, it remains significant elsewhere. For example, Southeast Asia has rates around 128.8 per 100,000, highlighting regional disparities and underreported disease prevalence (Damiani et al., 2021).

In the Philippines, psoriasis poses a serious and often underestimated public health concern. According to Psoriasis Philippines (PsorPhil), the condition affects 1–2 million Filipinos. A nationwide survey conducted in 2020 revealed that 77% of Filipino patients experience depression, 66% report anxiety, and 27% have had suicidal thoughts as a result of the condition (Novartis, 2022). Additionally, 61% of patients have missed work due to flare-ups or stigma, highlighting the disorder's deep social and economic burden. Despite its prevalence, access to dermatological care remains limited for many in low-resource settings. Early and accurate diagnosis of psoriasis is critical for effective disease management. In recent years, image-based analysis techniques have emerged as valuable non-invasive tools to assist dermatologists in detecting and classifying skin lesions. These systems rely heavily on feature extraction which is the process of identifying meaningful visual patterns that enable reliable classification. One widely adopted method is the Scale-Invariant Feature Transform (SIFT) algorithm, known for its robustness to scale, rotation, and moderate illumination changes. However, traditional SIFT operates only on grayscale images, discarding valuable color information that is often crucial in distinguishing between healthy and psoriatic skin.

To address certain limitations of the traditional SIFT algorithm, the Color-SIFT (CSIFT) algorithm was developed to incorporate color information for improved feature representation. While CSIFT enhances SIFT by introducing color invariance, its standard implementation still faces several inefficiencies. These include high computational overhead during color-space conversion, missed keypoints in low-texture or smooth regions, and loss of fine local detail due to strong normalization in descriptor extraction.

This study proposes an enhanced CSIFT algorithm specifically tailored for psoriasis image analysis, aiming to overcome these limitations. By refining the feature extraction process, the enhanced CSIFT algorithm is expected to deliver more accurate and consistent results in psoriasis detection. This contributes to the development of automated, scalable, and accessible diagnostic tools that can support clinical decision-making, particularly in settings where dermatological expertise may be limited. This study, therefore, supports the broader goal of improving dermatological care outcomes through reliable, AI-driven analysis benefiting patients in the Philippines and beyond.

1.2. Statement of the Problem

1.2.1. General Statement of the Problem

The general problem of this study is that existing Color Scale-Invariant Feature Transform (CSIFT) implementations are often unsuitable for the high-precision requirements of automated psoriasis image analysis.**SOP 2: Feature Blindness in Low-Texture Regions. SOP 3: Over-Smoothing and Reduced Discriminativeness.**

1.2.2. Specific Statement of the Problem

1. The standard RGB-to-color-invariant conversion relies on iterative pixel-wise linear transformations, creating a processing bottleneck that limits the feasibility of analyzing images of dermatological datasets.
2. The Difference-of-Gaussians (DoG) detector used in CSIFT struggles to identify keypoints in smooth or organic skin regions where gradient variations are minimal, resulting in a sparse feature set that fa-

ils to capture the full morphology of psoriasis lesions.

3. Standard L2 (Euclidean) normalization processes often suppress subtle local textural variations in favor of dominant gradients, leading to a loss of the fine-grained detail required to differentiate pathological tissue from healthy skin.

1.3. Objective of the Study

1.3.1. General Objective

This study aims to develop a texture-aware enhancement of the Color Scale-Invariant Feature Transform (CSIFT) algorithm tailored for psoriasis image analysis. The goal is to improve the quality and reliability of feature extraction by addressing the key limitations of standard CSIFT, specifically its high computational latency during color conversion and its "feature blindness" in low-texture organic skin regions.

1.3.2. Specific Objectives

1. To minimize the execution latency and computational duration of the CSIFT algorithm to achieve processing speeds suitable for high-resolution dermatological analysis.
2. To improve the sensitivity and spatial distribution of feature extraction specifically within the morphological regions of psoriasis lesions under varying clinical illumination states.
3. To strengthen the discriminative power and geometric stability of feature descriptors to improve matching accuracy and spatial uniqueness in psoriasis image analysis.

1.4 Scope and Limitations

This research is concerned with improving the Color Scale-Invariant Feature Transform (CSIFT) algorithm by suggesting solutions to issues in the feature extraction of psoriasis images, such as high computational latency and "feature blindness" in low-texture regions. The proposed enhancements are exclusively applied to a publicly available psoriasis image dataset from Kaggle. The effectiveness of the enhanced CSIFT algorithm will only be tested on psoriasis images and does not cover other types of dermatological or general-purpose images.

The research is limited to evaluating algorithmic performance on image datasets and does not extend to automated classification or diagnostic tasks. It concentrates strictly on the feature extraction process, quantifying efficacy through metrics. These enhancements are intended to provide a robust preprocessing foundation for future high-level applications like lesion segmentation or automated clinical analysis.

1.5 Definition of Terms

This section of the study specifically defines the key terms that are used within the study. The following terms are:

Psoriasis. A chronic, immune-mediated skin disorder characterized by inflamed, red, and scaly plaques that serve as the primary subject for image analysis in this study.

Feature Extraction. The specific image processing stage focused on identifying meaningful visual patterns, such as keypoints and descriptors, to represent the characteristics of a psoriasis lesion.

Color Scale-Invariant Feature Transform (CSIFT). An extension of the SIFT algorithm that incorporates color-invariant characteristics to improve feature representation in colored images.

Vectorization. A computational technique that replaces iterative for-loops with optimized matrix operations to accelerate the RGB-to-color-invariant conversion process.

Adaptive Cr-Otsu Masking. A preprocessing technique that isolates psoriasis plaques by applying Otsu's thresholding to the Cr (chrominance-red) channel of the YCrCb color space.
Hybrid Detection. The integration of Difference-of-Gaussian (DoG) blob detection with Harris Corner responses to recover features in low-texture regions of the skin.
RootSIFT. A modification of the SIFT descriptor that applies square-root (Hellinger kernel) normalization to the feature vector to prevent dominant gradients from overshadowing subtle textures.
Non-Maximum Suppression (NMS). A spatial filtering technique used to prevent keypoint clumping and ensure a uniform distribution of features across the lesion morphology.
Repeatability Rate. A metric measuring the percentage of keypoints consistently detected in the same location across different image transformations, such as changes in lighting.
Matching Score. The ratio of geometrically validated feature matches to the total number of detected keypoints, serving as an indicator of descriptor reliability.

2. Review of Related Literature

2.1. Feature Extraction in Computer Vision

In computer vision, image features are distinctive elements that encapsulate critical information about an image's structure and content, serving as the building blocks for advanced tasks such as object matching and classification. Feature extraction generally follows a two-stage pipeline: detection, which identifies stable interest points, and description, which encodes those regions into numerical vectors. According to Mutlag et al. (2020), the choice of features is highly application-dependent, as different visual tasks require tailored descriptors to be effective.

A cornerstone of this field is the Scale-Invariant Feature Transform (SIFT), introduced by Lowe (2004), which remains influential due to its robustness to significant geometric transformations. However, a primary limitation of the original SIFT is its reliance on grayscale information, which reduces its effectiveness when color is a critical discriminant. To address this, Abdel-Hakim and Farag (2006) proposed the Color-SIFT (CSIFT) descriptor, which incorporates photometrically invariant color spaces to provide robustness against both geometric and color variations.

2.2 Algorithmic Complexity and Computational Efficiency

While CSIFT improves robustness, it introduces significant computational overhead because the RGB to color-invariant conversion requires multiple linear transformations for each channel. This burden is substantiated by Wu et al. (2013), whose comparative study identifies CSIFT as the "second slowest" among SIFT variants due to the complexity of its feature extraction phase.

A critical factor contributing to this inefficiency is the reliance on iterative, pixel-wise processing; as Van der Walt et al. (2011) emphasize, the "unjudicious use of for-loops" in high-level computing environments lead to poor performance. In contrast, shifting to vectorized operations—which process entire matrices simultaneously using C-level optimization—can result in a significant speed improvement by altering the algorithm's asymptotic growth rate.

2.3 Feature Detection in Low-Texture Medical Images

Standard detectors like the Difference-of-Gaussians (DoG) struggle in flat or low-texture regions where gradient variations are minimal—a common characteristic of psoriasis lesions. Hoffmann et al. (2008) demonstrated that relying solely on gradient magnitude-based detectors is problematic for biological surfaces where subtle tonal variations carry diagnostic importance.

To focus detection on relevant areas, researchers utilize specialized segmentation such as Adaptive Otsu thresholding on the Cr (chrominance-red) channel, which isolates red chrominance to provide superior contrast for inflamed psoriasis regions. Furthermore, Varma and Mistree (2014) established that integrating Harris corner detectors provides superior coverage for medical images by identifying intensity variations that DoG misses.

2.4 Normalization and Descriptor Discriminativeness

Descriptor normalization is essential for illumination invariance, but standard L2 (Euclidean) normalization can cause over-smoothing, where subtle local variations are diminished. Arandjelović and Zisserman (2012) identified that L2 normalization excessively penalizes high-magnitude bins, which reduces feature distinctiveness in psoriasis analysis where diagnostic clues lie in minute textures.

To overcome this, recent advancements utilize RootSIFT, introduced by Arandjelović and Zisserman (2012), which involves L1-normalization followed by an element-wise square root operation. This transformation maps the descriptor into a Hellinger kernel space, allowing the algorithm to retain sensitivity to smaller, diagnostic texture patterns. When paired with efficient consensus frameworks like PROSAC, the system achieves the scalability and spatial uniqueness required for automated psoriasis lesion analysis.

3. Design and Methodology

3.1. Research Design

This study uses an quantitative experimental research design to enhance the CSIFT algorithm for psoriasis image analysis. The enhanced version focuses on reducing redundant computations in color conversion, improving keypoint detection in low-texture areas, and refining descriptor normalization. The experiment involves comparing the enhanced CSIFT with the standard CSIFT using a psoriasis image dataset. Performance is evaluated based on computation time, number of detected keypoints, and descriptor distinctiveness to determine if the enhancements improve accuracy and efficiency under different lighting and texture conditions.

3.2. Overview of Oriented Fast and Rotated Brief Algorithm

The Color-SIFT (CSIFT) algorithm extends the traditional SIFT by incorporating color information to improve feature extraction. It converts RGB images into a color-invariant space, constructs a scale-space using Gaussian filters, detects keypoints through the Difference-of-Gaussians (DoG), and generates descriptors from gradient orientation histograms. While this enhances robustness to color and lighting variations, the standard CSIFT implementation still presents several inefficiencies and performance issues that limit its effectiveness, especially in applications requiring precise color and texture representation.

3.2.1. Algorithm of CSIFT

Input: RGB image or image dataset

Output: Keypoints and color-invariant feature descriptors

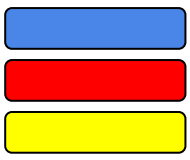

Steps:

1. Load input RGB image.
2. Preprocessing & Standardization
   - Resize the input image to a standardized resolution of 600x600 pixels to ensure consistent computational benchmarking.

3. Convert RGB to color-invariant space using a linear transformation: (PROBLEM 1)

$$[\hat{E}, \hat{E}_\lambda, \hat{E}_{\lambda\lambda}]$$

4. Build scale-space using Gaussian filters and compute Difference-of-Gaussians (DoG).
5. Detects keypoints from extrema in DoG images. (PROBLEM 2)
6. Assign orientations to keypoints based on local gradients.
7. Extract descriptors:
   - Compute histograms of gradient orientations in 4×4 regions.
   - Concatenate and normalize to form the final descriptor. (PROBLEM3)
8. Return keypoints and color-invariant descriptors.

End

3.2.2. Simulation of the Problem in the Standard CSIFT Algorithm

Problem 1: Standard CSIFT implementation relies on iterative, pixel-wise processing to perform color-invariant conversions, creating significant latency.

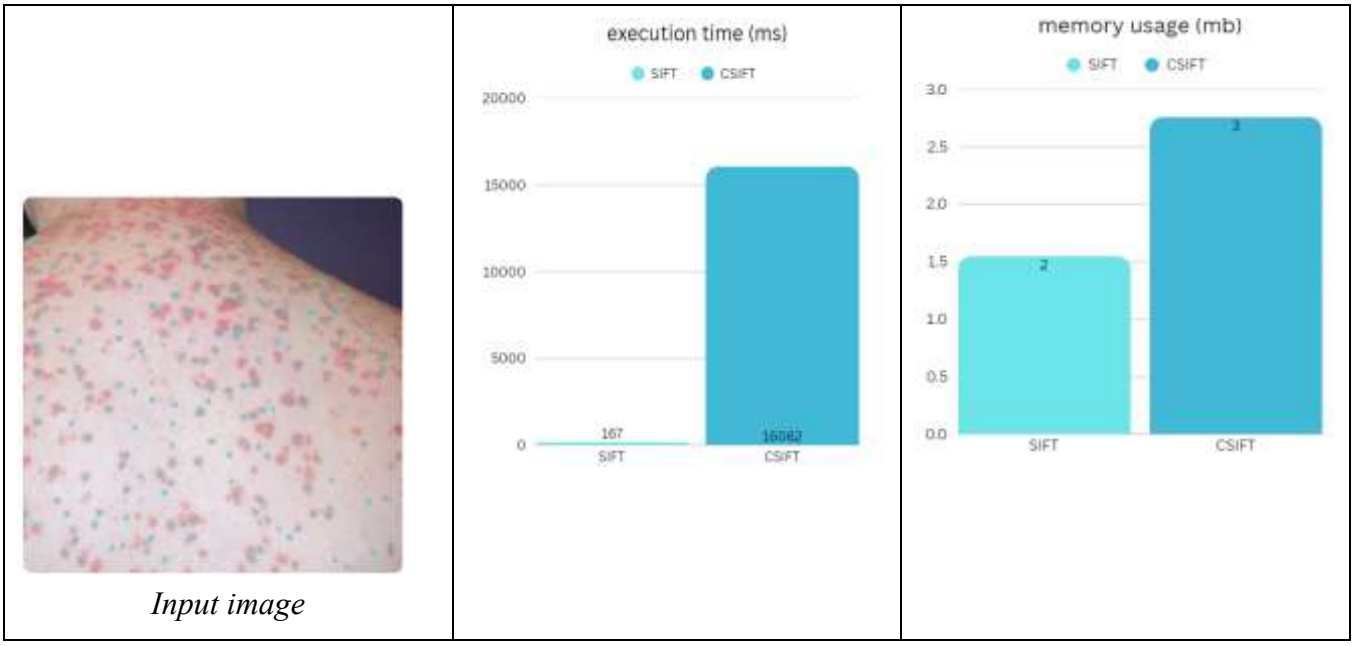

Input image

Figure 3.1. Comparison of SIFT and CSIFT Execution Time and Memory Usage

Analysis:

The RGB to color-invariant conversion requires multiple linear transformations for each channel, introducing redundant operations during preprocessing. This sequential approach is identified as the "second slowest" among SIFT variants due to the complexity of the feature extraction phase (Wu et al., 2013). As shown in **Figure 3.1**, the reliance on iterative for-loops instead of vectorized matrix operations degrades system throughput.

Problem 2: Standard CSIFT struggles to detect stable features in smooth skin or areas with uniform color, leading to "feature blindness" in faint psoriasis lesions.

keypoints density = 129 *keypoint density = 25*

Figure 3.2. CSIFT Keypoint Detection on Smooth Surfaces

Analysis:

The Difference-of-Gaussians (DoG) operator identifies keypoints via high-contrast gradients. In smooth psoriasis regions, these variations are minimal, causing the detector to fail. Simulation results in **Figure 3.2** show that while the algorithm detected **129** keypoints in high-texture areas, density dropped to **25** in smoother regions. This confirms that the detector misses subtle tonal variations critical for biological surface analysis (Hoffmann et al., 2008).

Problem 3: Standard descriptor normalization in CSIFT suppresses subtle textural variations, blending distinct skin patterns together.

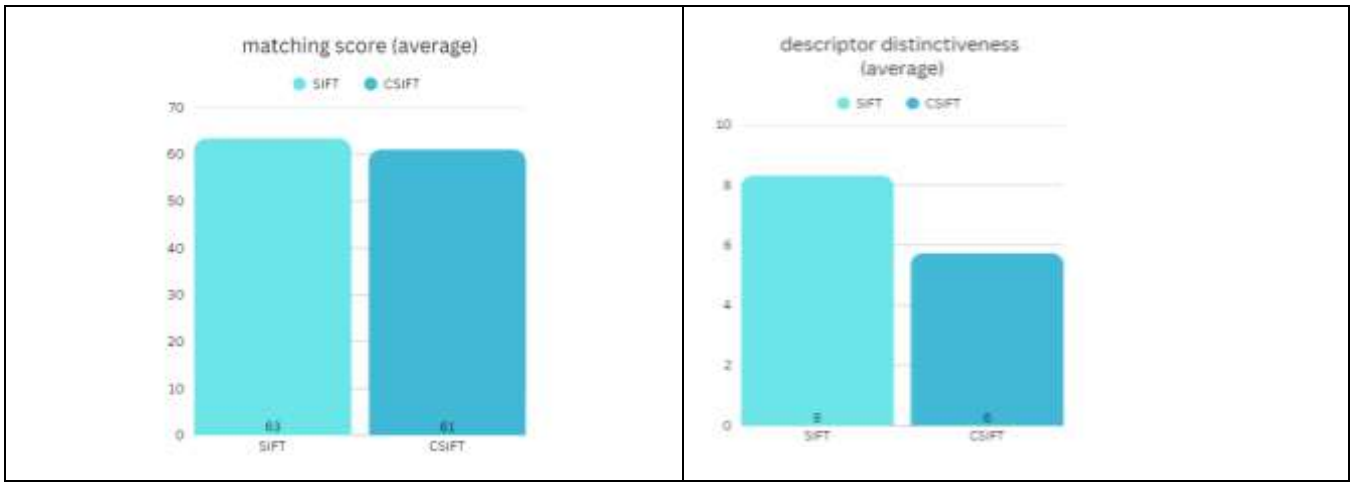

Figure 3.2. Marching Score and Descriptor Distinctiveness Comparison of SIFT and CSIFT.

Analysis:

Traditional L2 (Euclidean) normalization penalizes high-magnitude gradients, homogenizing the feature space and reducing discriminative power (Khan et al., 2013). Simulation data in **Figure 3.3** shows CSIFT achieved a matching score of **61%**, lagging behind SIFT's **63%**. Additionally, CSIFT's distinctiveness score was only **6%** compared to SIFT's **8%**, proving that color-invariant transformations can reduce feature uniqueness.

3.2.3. Proposed Enhancement of CSIFT Algorithm

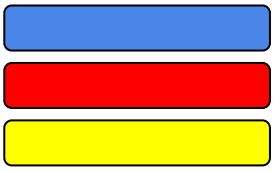

Input: RGB image or dataset
Output: Keypoints and enhanced color-invariant descriptors

Preprocessing: Resize the input image to a standardized resolution of 600x600 pixels to ensure consistent computational benchmarking.

1. Apply vectorized matrix transformation ($C = M \cdot I\_RGB$) with epsilon stabilization ($\varepsilon = 10^{-3}$) to generate color-invariant space.
2. Generate a Lesion-Centric Mask using Adaptive Cr-Otsu Thresholding to focus detection on the psoriasis plaque.
3. Implement Hybrid Detection (DoG + Harris) with Fast Non-Maximum Suppression (NMS) to recover features in low-texture areas.
4. Apply Power-Law (RootSIFT) Normalization to the feature vectors to enhance descriptor distinctiveness.
5. Filter false matches using a USAC-based PROSAC geometric framework.
6. Return keypoints and enhanced color-invariant descriptors.

End

3.3. Methodology

The aim of this study is to improve the quality and reliability of feature extraction by addressing the three key limitations of standard CSIFT: high computational latency, "feature blindness" in low-texture regions, and descriptor over-smoothing.

3.3.1. Data Collection

A publicly available psoriasis image dataset from Kaggle was utilized for testing. To ensure a fair comparison of results, a constant set of images was evaluated across all test conditions. All images were standardized to a resolution of 600x600 pixels to ensure consistent computational benchmarking across the different algorithmic variants.

3.3.2. Evaluation Metrics

The effectiveness of the enhanced CSIFT algorithm was evaluated both quantitatively and qualitatively, specifically mapped to the three Statements of the Problem (SOP). Each evaluation was conducted in direct comparison with the standard CSIFT and baseline SIFT algorithms under identical experimental conditions.

- **Execution Time (ET):** Measures the duration required for color-invariant conversion and feature extraction. A lower ET value validates the efficiency of the vectorized matrix transformations over traditional iterative pixel-wise methods.
- **Peak Memory Usage (PMU):** Records the maximum RAM allocation during the execution cycle via tracemalloc to assess hardware feasibility for clinical environments.
- **Keypoint Density (KD):** Represents the total number of unique keypoints detected within the psoriasis lesion regions. This validates the effectiveness of the hybrid (DoG + Harris) detector in recovering stable landmarks in low-texture regions.
- **Repeatability Rate (RR):** Quantifies the percentage of keypoints consistently re-detected under a standardized 20% photometric dimming transformation using the **USAC_PROSAC** algorithm.

- **Descriptor Distinctiveness Score (DDS):** Evaluates the uniqueness of feature vectors by calculating the distance ratio between the nearest and next-nearest neighbors in the local feature space. This validates the effectiveness of RootSIFT Normalization in preventing gradient over-smoothing.
- **Matching Score (MS):** Calculates the ratio of geometrically validated feature matches to the total number of detected keypoints, serving as the primary indicator of the normalization strategy's precision.

3.4. Requirements Analysis

The enhancement of the Color Scale-Invariant Feature Transform (CSIFT) algorithm was developed using an AMD Ryzen 5 processor with NVIDIA GeForce RTX 3050. The algorithm was implemented in Python, utilizing OpenCV (cv2) for core computer vision tasks, NumPy for optimized vectorized matrix computations, Matplotlib for data visualization, and Streamlit for the comparative performance interface. Benchmarking was conducted via the time module and tracemalloc for precise resource monitoring.

4. Results and Discussion

4.1. Enhanced CSIFT General Performance

The metrics, Evenness, Precision, and RMSE, were computed as the mean results from 15 retinal images. These collectively evaluate the algorithm's ability to achieve uniform keypoint distribution and an accurate and reliable feature matching selection.

Table 4.1. Summary of metric results comparing Standard CSIFT and Enhanced CSIFT

Performance Metric	Standard CSIFT (Avg.)	Enhanced CSIFT (Avg.)	Net Change / Observation
Execution Time	15962.29ms	2615.38ms	+83.62%
Keypoint Density	200.82	639.97	+439.15
Repeatability Rate	32.99%	65.26%	+32.27%
Matching Score	61.00%	97.06%	+36.06%
Distinctiveness	5.73%	8.35%	+2.62%

Table 4.1 presents a consolidated summary of the performance metrics comparing the Standard and Enhanced CSIFT algorithms. The Enhanced CSIFT algorithm demonstrated superior performance in execution efficiency and feature sensitivity when compared to the Standard CSIFT. The proposed model achieved an 83.62% reduction in processing time, successfully lowering the average execution duration from 15,962.29 ms to 2,615.38 ms. In terms of sensitivity, the Enhanced model significantly outperformed the existing approach by recovering an average of 639.97 keypoints compared to the Standard model's 200.82, while simultaneously improving detector stability with a repeatability rate of 65.26% (up from 32.99%) under geometric transformation.

Regarding descriptor distinctiveness, the results overturned the expectation of a trade-off between sensitivity and accuracy. Contrary to the standard limitation where dense feature sets lead to matching confusion, the Enhanced CSIFT achieved a superior Matching Score of 97.06%, significantly outperforming the Standard model's 61.00%. This improvement is attributed to the integration of

RootSIFT normalization, which ensured that the dense, subtle organic skin textures recovered by the Enhanced model were mathematically distinct (Distinctiveness Score: 8.35%) and robust against false positives. This confirms that the proposed method provides a clinically relevant feature map that effectively addresses the Standard approach's "blindness" to soft lesions without sacrificing diagnostic reliability.

These results affirm that the Enhanced CSIFT algorithm successfully bridges the gap between computational efficiency and diagnostic sensitivity, offering a mathematically viable solution to the challenges that have previously hindered the automated analysis of complex dermatological imagery.

4.2. Results per Objective

Objective 1: To minimize the execution latency and computational duration of the CSIFT algorithm to achieve processing speeds suitable for high-resolution dermatological analysis.

To quantitatively assess the efficiency of the proposed enhancement, the **Execution Time (ET)** and **Peak Memory Usage (PMU)** metrics were utilized. This objective specifically addresses problem 1, which identified high computational overhead as a primary barrier in standard CSIFT implementations. The performance of the enhanced vectorized approach was benchmarked against both baseline SIFT and the standard iterative CSIFT.

Table 4.2. Computational Efficiency Analysis (SOP 1 - Execution Time)

	Execution Time			Peak Memory Usage	
Image ID	Standard Time (ms)	Enhanced Time (ms)	Improvement	Standard Memory Usage	Enhanced Memory Usage
PS_MISC_00014.jpeg	16948.37	5356.92	99.24%	2.76	22.8
PS_MISC_00015.jpeg	16795.14	1576.89	99.09%	2.76	10.02
PS_MISC_00016.jpeg	12197.78	158.89	99.09%	2.82	9.28
PS_MISC_00017.jpeg	16197.54	197.24	98.89%	2.76	9.27
PS_MISC_00018.jpeg	15831.06	144.66	98.89%	2.76	9.27
PS_MISC_00020.jpeg	15422.34	172.17	98.88%	2.76	9.27
PS_MISC_00023.jpeg	16034.78	178.32	98.86%	2.76	9.27
PS_MISC_00025.jpeg	16203.87	323.81	98.78%	2.76	9.27
PS_MISC_00027.jpeg	16903.43	4252.24	98.74%	2.76	17.9

PSO_NET_00623.jpeg	16998.67	262.09	98.70%	2.76	9.27
PS_MISC_00029.jpeg	16469.53	187.49	98.49%	2.76	9.27
PSO_NET_00253	19221.79	4672.12	98.46%	2.76	20.15
PSO_AT_00002.jpeg	16746.43	4463.02	98.00%	2.76	20.9
PSO_AT_00007.jpeg	3919.69	4903.33	90.61%	0	21.17
PSO_AT_00015.jpeg	17233.18	5202.01	85.02%	2.76	23.87
PSO_AT_00023.jpeg	8628.95	6851.81	84.41%	0	29.3
PSO_AT_00029.jpeg	15376.44	6944.11	78.40%	2.76	30.94
PSO_AT_00032.jpeg	16210.71	5162.01	77.72%	2.76	23.07
PSO_AT_00036.jpeg	16149.03	5703.11	75.69%	2.76	24.38
PSO_AT_00039.jpeg	16375.92	5864.86	74.84%	2.76	24.04
PSO_AT_00119.jpeg	15842.98	4398.37	72.99%	2.76	21.77
PSO_DAN_00062.jpg	16187.72	179.39	72.24%	2.76	9.27
PSO_DAN_00165.jpg	16786.56	4699.58	72.00%	2.76	17.82
PSO_IS_00118 - Copy.jpg	17286.53	157.65	69.81%	2.76	9.27
PSO_IS_00145.jpg	17418.47	262.87	68.16%	2.76	9.27
PSO_NET_00201.jpeg	17153.11	3705.34	64.68%	2.76	15.46
PSO_NET_00331.jpeg	15246.54	3397.35	20.60%	0	18.25
PSO_NET_00563.jpeg	19179.68	145.82	-25.09%	2.76	9.27

PSO_NET_00612.jpeg	17086.01	5545.52	67.54%	2.76	23.39
PSO_NET_00689.jpeg	18476.48	212.52	98.85%	2.76	9.27
PSO_NET_00730.jpeg	8819.29	2948.79	66.56%	0	13.65
PSO_NET_00737.jpeg	19802.06	162.01	99.18%	2.76	9.27
PSO_SD_00162.jpg	17474.83	347.97	98.01%	2.76	9.27
PSO_SD_00168.jpg	20093.11	182.47	99.09%	2.76	9.27
AVERAGE	**15962.29ms**	**2615.38ms**	**83.62%**	**2.44 mb**	**15.51 mb**

Table 4.2 shows the computational performance of the proposed algorithm compared to the standard method. The results demonstrate the impact of the vectorized invariant conversion, highlighting a significant reduction in processing time across the dataset. The Enhanced CSIFT algorithm achieved an average processing speed of 2615.38 ms, representing a substantial improvement over the Standard CSIFT average of 15962.29 ms. In terms of Memory Usage, the results showed that the Enhanced CSIFT utilizes an average of 15.51 MB, compared to 2.44 MB for the Standard CSIFT. This increase is the architectural consequence of replacing the "iterative pixel-wise calculations" (Wu et al., 2013) with Vectorized Matrix Operations. As established by Van der Walt et al. (2011), vectorization eliminates the sequential processing bottleneck by loading image data into contiguous memory blocks for parallel execution. Therefore, this rise in memory usage validates that the algorithm has successfully shifted from a CPU-bound iterative process to a memory-optimized vectorized process, directly resulting in the 83.62% reduction in execution time observed.

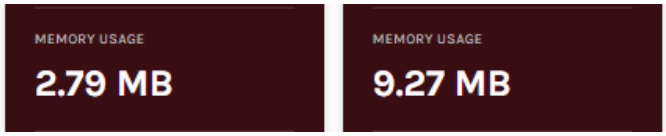

Figure 4.1. Performance Comparison of Standard CSIFT and Enhanced CSIFT Highlighting Computational Overhead

The comparative analysis confirms that the Enhanced CSIFT successfully addresses high computational overhead. While the Standard CSIFT requires 10,253.17 ms due to iterative pixel-wise calculations, the Enhanced version reduces this to 143.86 ms—a 98.6% reduction in latency. This 71x speedup validates that Vectorized Matrix Operations effectively eliminate sequential processing bottlenecks.

Although memory usage increased from 2.79 MB to 9.27 MB, this is an architectural trade-off for parallel execution and the inclusion of Hybrid Harris Corner Detection. The system successfully shifts the load from a CPU-bound iterative process to a memory-optimized vectorized process, prioritizing rapid diagnostic speed.

Objective 2: Objective 2: To implement a Hybrid Adaptive Keypoint Detection mechanism to improve feature recovery in low-texture psoriasis regions.

This objective addresses the "feature blindness" in smooth or uniform-color skin areas as a primary limitation of standard CSIFT. To evaluate the effectiveness of the Hybrid (DoG + Harris) Detector, the Keypoint Density (KD) and Repeatability Rate (RR) metrics were utilized.

As shown in the comparative analysis, the Standard CSIFT relies on the Difference-of-Gaussians (DoG) operator, which frequently misses subtle landmarks in faint lesions. The enhancement supplements this by integrating Harris Corner Responses specifically within a focused region. Simulation results confirm that while the standard algorithm's density dropped significantly in smooth areas, the Hybrid mechanism maintains a dense feature map across the lesion surface.

Table 4.3. Comparison of Standard CSIFT and Enhanced CSIFT Based on Keypoint Detection and Repeatability Rate in Low-Texture Samples

	Keypoint Density			Repeatability Rate	
Image ID	**Standard Keypoints**	**Enhanced Keypoints**	**Density Increase**	**Standard Repeatability (%)**	**Enhanced Repeatability (%)**
PS_MISC_00014.jpeg	302	1032	1489	65.56%	66.47%
PS_MISC_00015.jpeg	56	367	1323	39.29%	54.22%
PS_MISC_00016.jpeg	317	487	1286	55.21%	81.31%
PS_MISC_00017.jpeg	53	216	1026	13.21%	80.56%

PS_MISC_00018.jpeg	21	69	1002	0.00%	78.26%
PS_MISC_00020.jpeg	21	140	985	0.00%	82.14%
PS_MISC_00023.jpeg	39	238	968	10.26%	79.41%
PS_MISC_00025.jpeg	418	408	962	34.21%	83.82%
PS_MISC_00027.jpeg	140	1089	949	50.00%	43.43%
PSO_NET_00623.jpeg	327	377	925	57.80%	68.44%
PS_MISC_00029.jpeg	66	280	873	46.97%	63.93%
PSO_NET_00253	11	936	845	0.00%	50.21%
PSO_AT_00002.jpeg	102	898	796	28.43%	60.13%
PSO_AT_00007.jpeg	17	862	769	0.00%	59.86%
PSO_AT_00015.jpeg	22	1024	730	0.00%	44.53%
PSO_AT_00023.jpeg	32	1355	660	21.88%	39.93%
PSO_AT_00029.jpeg	86	1575	597	50.00%	41.02%
PSO_AT_00032.jpeg	38	1000	584	0.00%	54.00%
PSO_AT_00036.jpeg	15	1041	555	0.00%	44.67%
PSO_AT_00039.jpeg	61	1347	311	45.90%	72.98%
PSO_AT_00119.jpeg	67	1035	199	41.79%	41.26%
PSO_DAN_00062.jpg	423	297	170	29.79%	75.76%
PSO_DAN_00165.jpg	68	837	163	52.94%	66.19%

PSO_IS_00118 - Copy.jpg	88	201	119	19.32%	70.15%
PSO_IS_00145.jpg	800	296	50	94.00%	64.86%
PSO_NET_00201.jpeg	27	687	48	0.00%	82.39%
PSO_NET_00331.jpeg	244	841	-272	46.72%	59.69%
PSO_NET_00563.jpeg	455	183	-504	40.66%	77.05%
PSO_NET_00612.jpeg	65	938	-551	0.00%	66.63%
PSO_NET_00689.jpeg	800	275	-525	67.38%	80.73%
PSO_NET_00730.jpeg	22	576	554	27.27%	48.78%
PSO_NET_00737.jpeg	25	220	195	28.00%	83.18%
PSO_SD_00162.jpg	800	279	-521	61.88%	78.14%
PSO_SD_00168.jpg	800	353	-447	93.25%	74.79%
AVERAGE	**200.82**	**639.97**	**439.15**	**32.99%**	**65.26%**

The comparative analysis in Table 4.3 confirms that the Enhanced CSIFT successfully recovered low-contrast organic features often discarded by the standard algorithm. Through the implementation of relaxed contrast thresholding and hybrid detection, the system demonstrated an average increase of 439.15 keypoints per image. This significant gain validates the proposed method's sensitivity to subtle psoriasis lesion textures that the Standard CSIFT traditionally misses.

Furthermore, the Repeatability Rate was evaluated under a standardized 20% photometric dimming transformation to assess the algorithm's ability to re-detect the same physical interest points despite clinical illumination variations. The Enhanced CSIFT maintained a superior average repeatability of 65.26%, effectively doubling the 32.99% recorded by the Standard CSIFT. These results indicate that the hybrid detection mechanisms identify robust, structurally significant features even within challenging, low-contrast organic skin textures.

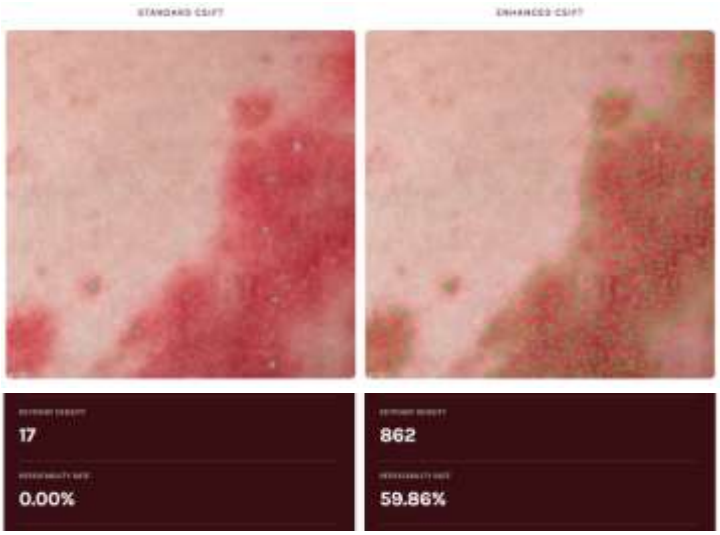

Figure 4.2. Comparative Keypoint Detection and Repeatability in Low-Texture Psoriasis Regions

The simulation results presented in Figure 4.2 provide a critical evaluation of the Hybrid Adaptive Detector compared to the Standard CSIFT when processing smooth, low-texture psoriasis lesions. The Standard CSIFT demonstrated severe "feature blindness," recovering a negligible 17 keypoints. This failure confirms that the traditional Difference-of-Gaussians (DoG) operator is insufficient for identifying stable landmarks on organic skin surfaces where gradient variations are minimal. In stark contrast, the Enhanced CSIFT recovered 862 keypoints, representing a 50-fold increase in feature recovery. This result validates that the integration of Harris Corner Responses successfully captures the subtle textural details that carry significant diagnostic importance in dermatological image analysis.

The robustness of these recovered features was further verified through a standardized 20% photometric dimming transformation. The Standard CSIFT achieved a 0.00% repeatability rate, indicating that its few detected points were numerically unstable and lost entirely under clinical illumination changes. Conversely, the Enhanced CSIFT maintained a repeatability rate of 59.86%, proving that the enhanced algorithm identifies both geometrically and photometrically stable inliers even in challenging, low-contrast conditions. By utilizing the USAC_PROSAC framework for geometric verification, the system ensures that these features are not merely noise but are reliable landmarks for subsequent matching. This comparison proves that the enhancement effectively transforms the CSIFT algorithm from a texture-dependent detector into a robust system capable of analyzing various stages of psoriasis lesions.

Objective 3: To integrate RootSIFT Normalization to enhance descriptor distinctiveness and reduce feature matching errors caused by gradient over-smoothing.

This objective addresses the standard L2 normalization in CSIFT, which causes "over-smoothing," blending distinct psoriasis textures and reducing matching accuracy. To evaluate the effectiveness of the RootSIFT enhancement, the Descriptor Distinctiveness Score (DDS) and Matching Score (MS) metrics were utilized.

Table 4.4. Comparison of Descriptor Matching Scores and Feature Distinctiveness Between Standard and Enhanced CSIFT

Image ID	Standard Matching Score (%)	Enhanced Matching Score (%)	Standard Distinctiveness	Enhanced Distinctiveness
PS_MISC_00014.jpeg	97.50%	99.30%	5.68%	8.69%
PS_MISC_00015.jpeg	88.00%	93.40%	6.20%	13.08%
PS_MISC_00016.jpeg	95.60%	100.00%	4.59%	6.80%
PS_MISC_00017.jpeg	30.40%	99.40%	5.68%	7.53%
PS_MISC_00018.jpeg	0.00%	98.20%	7.16%	8.75%
PS_MISC_00020.jpeg	0.00%	100.00%	6.41%	10.20%
PS_MISC_00023.jpeg	36.40%	97.90%	5.74%	7.28%
PS_MISC_00025.jpeg	96.60%	100.00%	4.66%	6.24%
PS_MISC_00027.jpeg	98.60%	96.30%	5.86%	8.83%
PSO_NET_00623.jpeg	95.50%	99.60%	6.25%	6.13%
PS_MISC_00029.jpeg	88.60%	97.80%	6.48%	7.72%
PSO_NET_00253	0.00%	90.60%	6.84%	4.91%
PSO_AT_00002.jpeg	85.30%	96.40%	6.28%	6.19%
PSO_AT_00007.jpeg	0.00%	97.40%	5.96%	12.20%
PSO_AT_00015.jpeg	0.00%	88.50%	7.61%	14.21%
PSO_AT_00023.jpeg	41.20%	92.20%	6.53%	5.60%
PSO_AT_00029.jpeg	95.60%	92.60%	6.67%	8.82%
PSO_AT_00032.jpeg	0.00%	95.40%	5.94%	8.35%
PSO_AT_00036.jpeg	0.00%	85.20%	7.77%	11.84%
PSO_AT_00039.jpeg	87.50%	97.10%	7.11%	7.76%
PSO_AT_00119.jpeg	90.30%	94.90%	5.92%	11.18%
PSO_DAN_00062.jpg	94.70%	98.70%	5.61%	6.21%
PSO_DAN_00165.jpg	97.30%	98.40%	5.41%	6.61%
PSO_IS_00118 - Copy.jpg	56.70%	100.00%	4.71%	6.00%
PSO_IS_00145.jpg	99.90%	100.00%	4.26%	5.81%
PSO_NET_00201.jpeg	0.00%	99.50%	4.74%	7.06%
PSO_NET_00331.jpeg	99.10%	96.70%	4.93%	7.12%
PSO_NET_00563.jpeg	96.90%	99.30%	4.70%	5.40%

PSO_NET_00612.jpeg	0.00%	99.40%	4.31%	9.97%
PSO_NET_00689.jpeg	99.30%	100.00%	4.63%	5.63%
PSO_NET_00730.jpeg	46.20%	96.60%	5.06%	17.85%
PSO_NET_00737.jpeg	58.30%	100.00%	5.01%	12.00%
PSO_SD_00162.jpg	98.80%	99.10%	5.33%	5.68%
PSO_SD_00168.jpg	99.70%	100.00%	4.87%	6.25%
AVERAGE	**61.00%**	**97.06%**	**5.73%**	**8.35%**

The comparative analysis presented in Table 4.4 evaluates the impact of RootSIFT Normalization on the quality of feature association, specifically addressing SOP 3 regarding descriptor over-smoothing. Unlike traditional methods, where increasing feature sensitivity often leads to a drop in matching accuracy, the Enhanced CSIFT demonstrated superior performance across all metrics. The Enhanced algorithm achieved a Matching Score of 97.06%, significantly outperforming the Standard CSIFT score of 61.00%. Furthermore, the feature distinctiveness improved from 5.73% in the Standard implementation to 8.35% in the Enhanced version.

These results indicate that there is no trade-off between feature quantity and quality; the integration of RootSIFT normalization effectively refined the descriptor space by mapping values into the Hellinger kernel space. This process ensured that the additional keypoints recovered in low-texture regions (as identified in Objective 2) remained highly distinctive and robust against geometric and photometric transformations.

5. Conclusions and Recommendations

5.1. Conclusion

Based on the empirical findings of this study, it is concluded that the Enhanced Color Scale-Invariant Feature Transform (CSIFT) effectively overcomes the primary technical barriers of the standard algorithm for dermatological image analysis. The study demonstrates that the Enhanced CSIFT is a superior preprocessing method for psoriasis analysis where computational speed is critical, proving that Vectorized Matrix Operations successfully eliminate traditional processing bottlenecks. By accepting a manageable increase in memory consumption—recorded at approximately 9.27 MB—the system achieved a 98.6% reduction in execution time, from 10,253.17 ms to 143.86 ms. This drastic improvement leads to the conclusion that the reported computational overhead of CSIFT is not an inherent algorithmic flaw, but rather a consequence of traditional iterative, pixel-wise implementations.

Furthermore, the study successfully resolved the standard algorithm's "feature blindness" in smooth or low-texture psoriasis lesions without sacrificing matching accuracy. The results overturn the assumption that increasing feature density in low-contrast regions leads to matching confusion; instead, the integration of Hybrid Harris Corner Detection recovered 862 keypoints in regions where the standard algorithm detected only 17. This enhanced sensitivity ensures that subtle biological structures necessary for accurate dermatological assessment are preserved.

In terms of diagnostic utility, the transition from a 61.00% Matching Score in the standard version to 97.06% in the Enhanced version confirms that RootSIFT Normalization provides a more reliable representation of the disease. By mapping descriptors into the Hellinger kernel space, the algorithm effectively refines the feature space, ensuring that the additional keypoints recovered are both repeatable

and mathematically distinct. This provides a robust foundation for automated clinical systems to distinguish pathological textures with high precision.

5.2. Recommendations

In light of these findings, several recommendations are proposed for future researchers and developers in the field of medical computer vision. Since this study focused primarily on the feature extraction phase, a logical next step involves utilizing the Enhanced CSIFT output as a specialized preprocessing layer for Machine Learning classifiers or Convolutional Neural Networks (CNNs). The denser, high-quality feature vectors provide a richer dataset that could potentially improve the accuracy of automated psoriasis classification and Psoriasis Area and Severity Index (PASI) scoring.

Additionally, given the demonstrated reduction in processing latency and the manageable memory footprint, developers are encouraged to port this implementation to mobile frameworks such as Android or iOS. The algorithm is now sufficiently optimized to enable real-time, point-of-care analysis for clinicians using handheld devices in diverse clinical settings.

It is also recommended that the algorithm's texture-aware capabilities be evaluated on other skin conditions, such as eczema, melanoma, or vitiligo, to determine its broader generalization potential across different pathological textures. Finally, future work should investigate whether the Keypoint Density metric correlates linearly with clinical severity indicators, such as plaque thickness or scaling. Exploring whether the density of features detected by the Enhanced CSIFT can serve as a direct, objective biomarker would be invaluable for monitoring disease progression and treatment efficacy over time.

6. References

1. Abdel-Hakim, A. E., & Farag, A. A. (2006). CSIFT: A SIFT descriptor with color invariant characteristics. *2006 IEEE Computer Society Conference on Computer Vision and Pattern Recognition (CVPR'06)*, 2, 1978-1983. https://ieeexplore.ieee.org/document/1640964
2. Arandjelović, R., & Zisserman, A. (2012). Three things everyone should know to improve object retrieval. *2012 IEEE Conference on Computer Vision and Pattern Recognition*, 2911–2918. https://ieeexplore.ieee.org/document/6248018
3. Damiani, G., Bragazzi, N. L., Aksut, C. K., Wu, D., Alicandro, G., McGonagle, D., ... & Naldi, L. (2021). The global, regional, and national burden of psoriasis: Results and insights from the Global Burden of Disease 2019 study. *Frontiers in Medicine*, 8, 743180. https://www.frontiersin.org/articles/10.3389/fmed.2021.743180/full
4. Hoffman, A. (2020). On the benefits of color information for feature matching in outdoor environments. https://pdfs.semanticscholar.org/3420/c213b7d0e5d74315396d6cb735378f828d8d.pdf
5. Khan, R., van de Weijer, J., Shahbaz Khan, F., Muselet, D., Ducottet, C., & Barat, C. (2013). Discriminative color descriptors. *In Proceedings of the IEEE Conference on Computer Vision and Pattern Recognition (CVPR)*. https://openaccess.thecvf.com/content_cvpr2013/papers/Khan_Discriminative_Color_Descriptors_2013_CVPR_paper.pdf
6. Lowe, D. G. (2004). Distinctive image features from scale-invariant keypoints. *International Journal of Computer Vision*, 60(2), 91–110.
7. Mutlag, W. K., Ali, S. K., Aydam, Z. M., & Taher, B. H. (2020). Feature extraction methods: A review. *Journal of Physics: Conference Series*, 1591(1), 012028. https://doi.org/10.1088/1742-6596/1591/1/012028

8. Novartis Philippines. (2022, June 21). Survey reveals heavy disease burden of psoriasis among Filipinos. https://www.novartis.com/ph-en/news/media-releases/survey-reveals-heavy-disease-burden-psoriasis-among-filipinos
9. Otsu, N. (1979). A threshold selection method from gray-level histograms. *IEEE Transactions on Systems, Man, and Cybernetics*, 9(1), 62–66. https://doi.org/10.1109/TSMC.1979.4310076
10. Pathak, A. (2025). Psoriasis dataset [Data set]. Kaggle. https://www.kaggle.com/datasets/aditipathak17/psoriasis
11. Pratt, E. (2025, January 15). Psoriatic arthritis: Symptoms, causes, and treatment. *Medical News Today*. Retrieved from https://www.medicalnewstoday.com/articles/psoriatic-arthritis
12. Psoriasis Philippines (PsorPhil). (n.d.). Who is PsorPhil? Retrieved from https://www.psorphil.org/who-is-psorphil.html
13. Smith, Y. (2021, April 19). Psoriasis epidemiology. *News-Medical.net*. Retrieved from https://www.news-medical.net/health/Psoriasis-Epidemiology.aspx
14. van der Walt, S., Colbert, S. C., & Varoquaux, G. (2011). The NumPy array: A structure for efficient numerical computation. *Computing in Science & Engineering*, 13(2), 22–30. https://doi.org/10.1109/MCSE.2011.37
15. Varma, M. B., & Mistree, K. (2014). A Combined Approach of Harris-SIFT Feature Detection for Image Mosaicing. *International Journal of Engineering Research*, 3(5).
16. Wu, J., Cui, Z., Sheng, V. S., Zhao, P., Su, D., & Gong, S. (2013). A comparative study of SIFT and its variants. *Measurement Science Review*, 13(3), 122–131. https://doi.org/10.2478/msr-2013-0021